

FUNCTIONAL ENHANCEMENT OF ENZYMATICALLY HYDROLYZED DOUBLE CROSSLINKED HOT MELT STARCH

Hao Wang, ChuanWei Zhang*

College of Mechanical and Electrical Engineering, Qingdao University, Qingdao 266071, Shandong, China.

Corresponding Author: ChuanWei Zhang, Email: zhangchuanwei3722@163.com

Abstract: In order to enhance the comprehensive performance of hot melt starch (TPS), in this study, a structurally stable TPS composite with excellent mechanical properties was prepared by using enzymatic-crosslinking composite as the core of modification, combined with organo-montmorillonite (OMMT) hybridisation strategy. The molecular weight of starch was reduced by α -amylase pretreatment to improve its fluidity; subsequently, citric acid and sodium trimetaphosphate were used for synergistic cross-linking to construct a dense three-dimensional molecular network structure, which enhanced the thermal stability and water resistance of the material. On this basis, different mass fractions of OMMT were introduced to further improve the mechanical strength and flexibility of the composite system through interfacial modulation. The results show that the appropriate amount of OMMT can effectively improve the tensile strength and elongation at break of the materials, and the performance is optimal when the amount of OMMT added is 1.5 g. The results show that the OMMT can be used in the composite system to improve the mechanical strength and flexibility of the materials. Excessive fillers, on the contrary, caused aggregation and weakened the enhancement effect. This study provides a new idea for the functionalized design of degradable starch materials, which is of positive significance to promote the practical application of TPS in packaging and biomedical fields.

Keywords: Hot melt starch; Enzymatic cross-linking; Montmorillonite hybridisation; Device design

1 INTRODUCTION

As human society's demand for environmentally friendly materials continues to rise, the ecological risks posed by traditional petroleum-based plastics, which are difficult to degrade, are a source of growing concern[1]. These synthetic materials are extremely stable in the natural environment, causing large amounts of 'white pollution' to remain in soil and water over time, posing a potential threat to ecosystems and human health[2]. In addition, the environmental costs of these materials are exacerbated by the non-renewable nature of petrochemical resources and the high carbon emissions generated during processing[3]. For this reason, the search for a sustainable alternative material that is both degradable and adaptable to the demands of modern industrial processing has become a key focus of current materials science research[4].

Starch, as a natural polysaccharide, is regarded as one of the most promising bio-based biodegradable polymers because it is not only widely available and inexpensive, but also can be rapidly decomposed into harmless substances under the action of microorganisms and enzymes[5]. However, the application of natural starch also faces a series of challenges, mainly in terms of its poor thermoplasticity[6], weak mechanical properties, and susceptibility to hygroscopicity, making it difficult to directly replace traditional plastics[7]. In actual processing, the melting temperature of starch is usually close to or exceeds its decomposition temperature[8], making it difficult to achieve industrial production by thermal processing[9]. Therefore, modification research around starch for structural adjustment and property optimisation has gradually become a key topic.

To address the thermal processing obstacles of natural starch, the concept of 'Thermoplastic Starch' (TPS) has been proposed in the academic community[10], which means that starch can exhibit processing characteristics similar to those of thermoplastic polymers[11] through the introduction of plasticisers and appropriate modification strategies[12]. Early thermoplastic modifications were mainly made by adding small molecules such as glycerol, urea, sorbitol, etc., to break the hydrogen bonds between the starch chains, thus imparting a certain degree of flexibility and processability to the material[13]. However, although plasticising modification improves the processing fluidity[14], it has limited enhancement on the mechanical strength and environmental stability of the material[15], especially under humid or high temperature conditions, and its mechanical properties still fluctuate greatly[16].

On this basis, researchers began to synergistically design the enzymatic degradation of starch with chemical cross-linking[17]. By controlling the degree of enzymatic degradation, the molecular weight and crystallinity of starch molecules can be effectively reduced[18], and the inter-chain entanglement can be reduced, thus enhancing its fluidity and lowering the melting threshold. Cross-linking modification, on the other hand, can build a stable three-dimensional network structure between the molecules, enhancing their mechanical support and thermal stability[19]. The combination of the two is expected to realise the goal of a material that is 'soft but strong', i.e., having good ductility and a certain degree of structural strength at the same time[20].

Among many enzymes, α -amylase is widely used in starch modification due to its high selectivity and mild reaction conditions[21]. Its mechanism of action is mainly to hydrolyse the α -1,4 glycosidic bond within the starch molecule[22], rapidly reducing the molecular chain length and providing more efficient reaction sites for the subsequent chemical modification reaction. In the cross-linking strategy, citric acid and sodium trimetaphosphate showed a good synergistic

effect in constructing the cross-linking network due to their high reactivity and environmental friendliness[23]. The former formed cross-links between starch chains through esterification to enhance its mechanical stability[24], while the latter further enhanced the consistency and density of the network structure through phosphoric acid esterification[25], which significantly improved the thermal stability and hydrolysis resistance of the material[26].

Although preliminary progress has been made in the enzymatic digestion and cross-linking of hot melt starch, there are still limitations in the single organic phase modification system[27]. For example, the modified TPS still suffers from water absorption and softening under high humidity environment[28], and there is still room for improvement of mechanical properties[29]. For this reason, the introduction of nano-organic fillers to form hybrid structures with starch has become a new research trend in recent years[30]. Layered inorganic materials, such as montmorillonite (MMT), have high specific surface area and excellent barrier properties[31], which can form a stable interface with starch through hydrogen bonding and electrostatic adsorption, significantly improving the rigidity and water resistance of the material[32]. In particular, organically modified montmorillonite (MMT-P) can further improve the compatibility with the organic matrix[33], enabling the composites to achieve good ductility and processing stability while maintaining high strength.

In addition, the nanohybrid fillers can also inhibit the thermal degradation behaviour of starch materials in thermal processing on a microscopic scale, improve their rheological stability, and expand their applications in high-temperature processes such as injection moulding and extrusion[34]. In recent years, TPS composites by constructing inorganic-organic hybrid interfacial structures have shown promising prospects in food packaging, disposables, and biomedical materials[35].

Based on the above background, this study proposes a novel TPS material preparation pathway based on enzymatic and cross-linking synergistic modification combined with inorganic montmorillonite hybridisation enhancement, aiming to comprehensively improve the thermoplastic processability, mechanical properties and environmental stability of starch-based materials. The research work will focus on the following aspects: (1) to explore the influence of the degree of enzyme digestion on the structure and plasticity of starch; (2) to analyse the regulation mechanism of different cross-linking agents on the network structure and physical properties of the materials; (3) to investigate the effect of OMMT on the microstructure, mechanical strength and moisture resistance of the composites with different additions; (4) to ultimately realise a functionalised hot-melt starch composite material with excellent comprehensive performance, and to provide a new pathway for the preparation of TPS materials. starch composites with excellent comprehensive performance, providing theoretical support and experimental basis for its industrial application in the field of green materials.

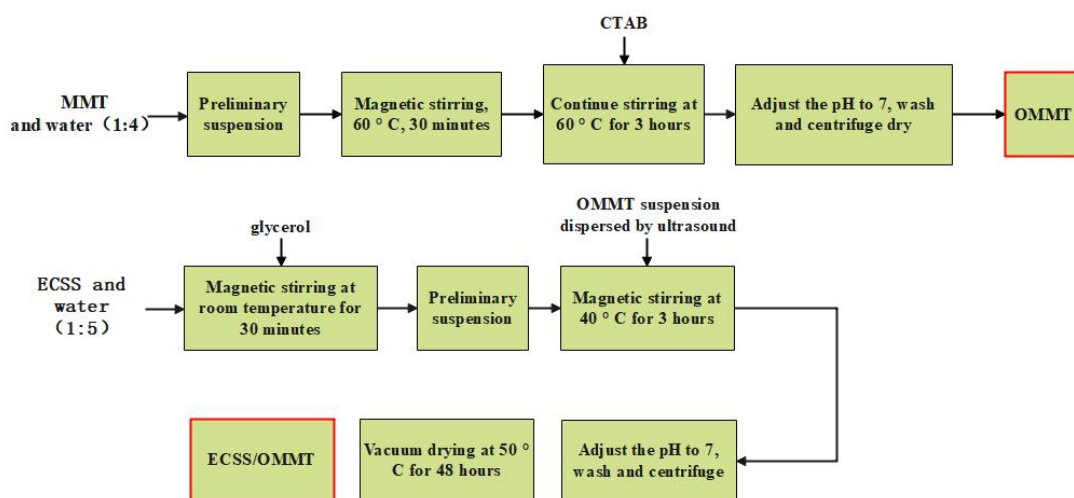


Figure 1 Modification of Organic Montmorillonite (OMMT) and Hybrid Process of ECSS and OMMT

2 MATERIALS AND METHODS

2.1 Experimental Material

The starches used in this experiment were common corn starch, medium temperature α -amylase (2 U/mg), hydrochloric acid, sodium hydroxide, urea, citric acid, sodium trimetaphosphate, montmorillonite, cetyltrimethylammonium bromide (CTAB), and ethanol (C₂H₆O) were purchased from the Macklin Company (Shanghai, China), and glycerol was purchased from the Shanghai Hutai Test.

2.2 Experimental Methods

2.2.1 Enzymatic double cross-linked starch preparation

Enzymatic starch preparation process: natural corn starch (20 g) and distilled water (80 g) were added to a round-bottomed beaker, and the material containing the experimental reaction was placed in a water bath with the temperature of the water bath set to 80°C, and the fully pasted starch was prepared by rapid stirring for 30 min under this environment. Next, 0.05 g of medium-temperature α -amylase was weighed into a beaker containing 10 ml of distilled water and stirred well to make an enzyme solution, which was added to the pasted starch, and then stirred rapidly at 80°C for five minutes to allow the pasted starch to begin to produce the obvious phenomena of liquefaction and thinning. Ice water was prepared in advance, and the liquefied starch solution was placed in the ice water for rapid cooling to stop the continued reaction of the amylase enzyme. After cooling to room temperature, the starch solution was adjusted to a pH <3 using a hydrochloric acid titration solution (1 mol/L), followed by continued manual stirring for 10 min. At the end of stirring, the beaker was placed in a water bath heated to 100°C for 5 min for enzyme inactivation, and after the heating was completed the flask continued to be transferred to ice water to vacate, and after the solution was brought down to room temperature, PH adjustment was carried out. The pH of the slurry was adjusted using sodium hydroxide solution (1mol/L), and the appropriate amount was dropped to react with the remaining hydrochloric acid in the solution, thus completing the inactivation of the enzyme. The reacted starch solution was poured into a polytetrafluoroethylene petri dish and put into a vacuum oven with the temperature set at 70°C for 24 h. The successfully modified enzymatic starch ES was obtained after the drying was completed.

Preparation of sodium citrate tri-metaphosphate double crosslinked starch (ECSS): firstly, 30 g of enzymatically dissolved starch (ES) was mixed with 100 mL of distilled water and stirred to form a homogeneous starch solution. Subsequently, glycerol (2 g) and urea (1 g) were added as plasticisers, and the pH was adjusted to 5.5 to provide suitable conditions for the esterification and cross-linking of citric acid. After adding 9 g of citric acid, the mixture was stirred and mixed well at room temperature, and then placed in a water bath at 70°C for 2 hours to promote the esterification of citric acid with the hydroxyl groups on the molecular chain of starch.

After the first step, the slurry was cooled to room temperature. Subsequently, the pH was adjusted to 10 with 1 mol/L sodium hydroxide solution to create a suitable environment for phosphate esterification with sodium trimetaphosphate. 9 g of sodium trimetaphosphate was added and placed in a water bath at 35°C for 2 h to achieve the second step of cross-linking, i.e., the phosphate bonding between sodium trimetaphosphate and the hydroxyl groups of starch.

After the reaction was completed, the sample was washed three times with a 1:1 mixture of distilled water and ethanol to remove unreacted cross-linkers and by-products. Subsequently, the pH of the system was adjusted to neutral using 1 mol/L hydrochloric acid solution. Finally, the treated slurry was poured into a polytetrafluoroethylene petri dish and vacuum dried at 40°C for 24 h to obtain the enzymatically cleaved citric acid/sodium trimetaphosphate double crosslinked modified starch samples (ECSS).

2.2.2 Preparation of organic montmorillonite (OMMT)

First, a preliminary suspension was prepared by adding 20 g of natural montmorillonite (MMT) to 100 mL of deionised water. The mixed system was stirred in a magnetic stirrer at a constant temperature of 60 °C for 30 min to promote uniform dispersion of the montmorillonite. Subsequently, an appropriate amount of cetyltrimethylammonium bromide (CTAB) was added to the system as an organic intercalating agent, and the reaction was continued for 3 h to insert organic cations into the interlayer structure of montmorillonite to achieve organic modification. After the reaction was completed, the pH of the system was adjusted to neutral and the products were washed several times using a mixture of ethanol and distilled water to remove unreacted impurities and surface adsorbates. Afterwards, the washed sample was centrifuged, and the supernatant was taken, poured into a polytetrafluoroethylene Petri dish, and dried in a vacuum oven at 60 °C for 24 h. The final organic modified montmorillonite (OMMT) powder was obtained in the form of flakes.

2.2.3 Preparation of thermoplastic starch/montmorillonite composites

Twenty g of dried double crosslinked enzymatically cleaved thermoplastic starch (ECSS) was mixed with 100 mL of distilled water, 2 g of glycerol was added as a plasticiser and the slurry was stirred in a magnetic stirrer for 30 min at room temperature to make the slurry well homogenised. Different masses of OMMT (0.5 g, 1.5 g, 3.5 g, and 5 g, respectively) were taken and mixed with a small amount of distilled water, and dispersed by ultrasonic dispersion using an ultrasonic processor (200 W, 10 min), with the aim of facilitating the exfoliation of the montmorillonite flake layer and improving the stability of its dispersion in the starch matrix. The ultrasonicated OMMT solution was slowly added to the ECSS slurry and stirring was continued for 3 h at 40 °C to promote the interaction and physical hybridisation between montmorillonite and starch molecules. The slurry obtained after the reaction was cleaned and transferred to a Teflon mould, and dried in a vacuum oven at 50 °C for 48 hours to obtain ECSS/OMMT composite samples with different OMMT contents. The samples were named MMT-1 (0.5 g), MMT-2 (1.5 g), MMT-3 (3.5 g) and MMT-4 (4.5 g) according to the amount of OMMT added.

2.2.4 Preparation of thin films

The dried ECSS/OMMT composite powder was placed into a mould lined with PTFE film on the top and bottom of the mould, and transferred to a hot pressing unit for moulding. The hot pressing conditions were set at a temperature of 50 °C and a pressure of 0.5 MPa, with a continuous pressure of 5 minutes, a holding pressure of 3 minutes, and a natural cold pressing of 20 minutes, after which the mould was removed to obtain a structurally intact hot-pressing moulded starch film.

2.3 Micro-Morphological Characterisation of Modified Starch

he prepared films were subjected to optical observation in a bright environment to observe the appearance and morphology of the films as well as the light transmittance and transparency of the films.

The film samples were subjected to gold sputtering and the internal structure of different hot-pressed starch films was observed using a scanning electron microscope (JEOL-JSM6400, Tokyo, Japan).

2.4 Fourier Transform Infrared Spectroscopy (FTIR)

The effect of modification on the chemical structure of starch films was analysed by Fourier Transform Infrared Spectroscopy analysis (FTIR; Nicolay iS20, Thermo Fisher Scientific, USA), where the film samples were analysed by FTIR using FTIR, with FTIR spectra of each sample taken in the range of 400 to 4000 cm^{-1} .

2.5 Thermogravimetric Analysis (TGA)

The thermal stability of the films was studied using a TAsDT650 simultaneous thermal analyser. The weight of the samples was about 5 mg and the heating temperature was set from room temperature to 450°C with the heating rate set at 10°C/min.

2.6 Mechanical Property Analysis

A universal mechanical testing machine (Instron 3367, Illinois Tool Works, Inc.) was used. The films obtained by hot pressing were cut with a sample length of 35 mm thickness of 1 mm and the tensile strength and elongation at break of the samples were measured. Five sets of tests were performed for each sample at room temperature and the average of the tests was taken.

2.7 Water Vapour Transmission (WVT)

WVT was measured using a modified version of the method ASTM E - 96-95. The sample films were cut and sliced into circles of 65 mm diameter and placed on a table at 50% humidity to obtain a constant weight. The experimental temperature was $23 \pm 2^\circ\text{C}$ with 50% humidity. And the weight of the disc assembly was taken every half an hour to obtain the weight reduction. The water vapour transmission rate was calculated by the following equation:

$$\text{WVT} = \frac{\Delta_m}{\Delta_t * S} \quad (1)$$

Δ_m is the amount of water subtracted, Δ_t is the experimental time, S is the film area.

2.8 Water Contact Angle Test

The film was placed horizontally on the experimental platform, 50 μL of distilled water was added each time, and the water contact angle was recorded by the software after the value was stabilised. Each sample was tested 5 times and the final contact angle was calculated as the average of the 5 measurements.

3 RESULTS AND DISCUSSION

3.1 Microstructure

The figure 1 shows the surface morphology evolution process of enzymatically crosslinked hot melt starch composite materials under different OMMT addition amounts. From Figure A, it can be seen that the ECSS sample without OMMT doping has a relatively flat film surface, but there are still a certain number of bubbles and small particles, resulting in poor film uniformity and insufficient surface density. Figure b shows the sample (MMT-2) with 1.5g of OMMT added, which has the most dense and smooth surface, significantly reduced wrinkled structure, significantly reduced number of bubbles, and no obvious agglomeration phenomenon. This indicates that OMMT has the best dispersion effect in the matrix and stable composite interface structure, making it the sample with the best surface quality among all groups. In Figure c, the amount of OMMT added was further increased to 3.5g. Although it still maintained a certain degree of uniformity, granular micro area distribution could be observed, indicating that the filler began to show local aggregation. As shown in Figure d, the OMMT increased to 5g, and the membrane surface became significantly rough, with a large number of agglomerates and protrusions. Surface defects increased significantly, and the hybridization degree became imbalanced, resulting in overall structural disorder of the membrane material. From this, it can be seen that an appropriate amount of OMMT (such as 1.5g) can significantly optimize the surface morphology of starch basement membrane, while excessive OMMT will destroy its structural uniformity and reduce material quality. The 1.5g OMMT group shown in Figure b is the composite sample with the best film-forming and surface density in this study.

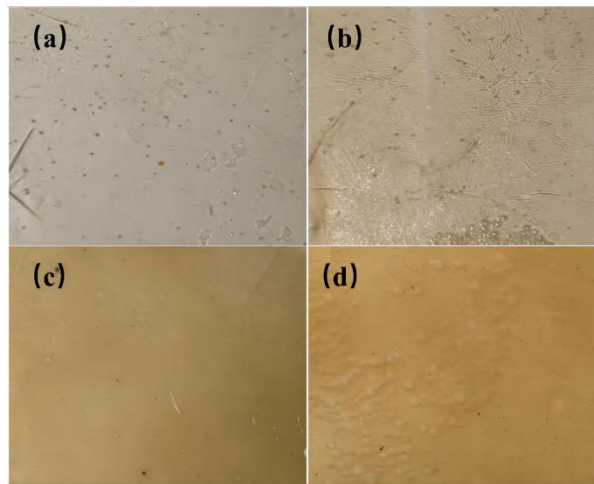


Figure 2 Comparison of Starch Hybrid Samples with Different Content of MMT:(a) MMT-1, (b) MMT-2, (c) MMT-3, (d) MMT-4

The scanning electron microscope (SEM) 200x images shown in Figure 2 visualise the effect of different content of organo montmorillonite (OMMT) doping on the cross-sectional microscopy of starch-based composites. The cross-sectional morphology of the films at different doping ratios showed significant differences, reflecting the important role of OMMT involved in the hybridisation process to regulate the densification and homogeneity of the materials.

In the MMT-1 sample corresponding to Figure (a), although some of the montmorillonite flakes have achieved initial dispersion in the matrix, the overall interface is still agglomerated, and more holes and irregular structures appear locally, indicating that the OMMT has not yet effectively established a continuous reinforcement network and the structure of the composite system is relatively loose under the low content condition. In contrast, the MMT-3 and MMT-4 samples shown in Figure (c) and (d) showed the problems of lamellar stacking and excessive overlapping, although the addition amount of OMMT was increased. The excessive stacking between the lamellae resulted in the internal structure of the material becoming inhomogeneous, accompanied by obvious cracks and particle aggregation, and the overall densification was instead damaged, which may weaken the mechanical and barrier properties of the material. Most notably, the MMT-2 sample shown in Figure (b) has a flat and homogeneous cross-sectional structure, with no obvious cracks or pores, and the film layer exhibits excellent continuity and densification. This morphology indicates that the appropriate amount of OMMT not only achieves good compatibility with the starch matrix, but also may form a stable synergistic structure with the starch chain segments at the molecular level, which effectively enhances the overall organisation and intermolecular forces of the material. At this time, the dispersion state of the lamellae is the most ideal, and the composite network can be fully formed, which provides a reliable basis for the mechanical enhancement and the improvement of barrier properties.

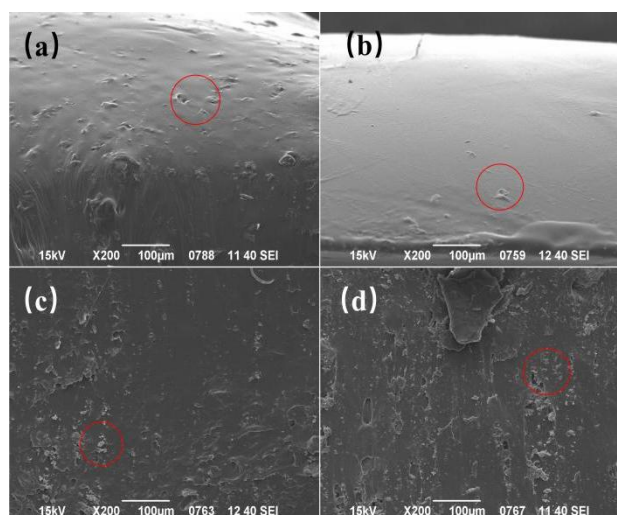


Figure 2 200x Electron Microscopy Structural Images of Different Samples: (a) MMT-1,(b) MMT-2, (c) MMT-3, (d) MMT-4

From the 1000× scanning electron microscope (SEM) images shown in Fig 3, different contents of organo-montmorillonite (OMMT) doping has an important influence on the microstructural distribution and hot-melt processing behaviour of composite thin film materials, which can indirectly reflect the material's fluidity, densification and structural stability during the hot-melt process.

Figure (a) (MMT-1) sample at low content of OMMT, the cross-section of the film layer can be seen obvious pores and irregular structure, the lamellae are not sufficiently peeled off, and some areas still exist agglomerates. This phenomenon suggests that during hot pressing, the material in the molten state has insufficient fluidity and fails to form a homogeneous and dense structure, resulting in insufficient spreading of the lamellae during thermoplastic processing and affecting the quality of the film formation.

Figure (c) and Figure (d) (MMT-3 and MMT-4) samples show the state of lamellar aggregation and dense microcracks, especially in Fig. (d) there are obvious lamellar stacking and cracks, which reflects that the uneven dispersion of OMMT in the high additive amount leads to the local structure of the 'bridge' effect, which limits the mobility of chain segments and the intermolecular structure of the material in the process of hot-melt. This reflects that the uneven dispersion of OMMT in high additive amount leads to the 'bridging' effect in the local structure, which limits the mobility of chain segments and intermolecular coordination ability of the material in the hot-melt process, and the phenomenon of 'melt fault' or internal cavity may appear in the hot-melt processing, which reduces the consistency of the overall film and processability.

In contrast, the cross-section of the sample in Figure (b) (MMT-2) is the flattest and densest, with almost no obvious holes and lamellar accumulation, showing good structural homogeneity and continuity. This structural morphology fully demonstrates that, under the appropriate doping ratio of OMMT, the material has good fluidity and dispersion properties during the hot-melt process, and a 'synergistic' micro-network may have been formed between OMMT and the starch matrix, which enables the starch chain segments to achieve a uniform orientation and distribution under the heated melt state, resulting in dense and continuous film structures. This feature also directly corresponds to the hot melt structure. This feature also directly corresponds to the improvement of the mechanical properties and film-forming quality of the samples obtained after hot-melt processing.

In summary, the 1000 \times SEM images not only reveal the microstructure regulation by the change of OMMT content, but also indirectly reflect the molecular movement and building ability of the material during hot-melt processing. Among them, the MMT-2 hybrid samples showed the optimal molecular structure arrangement and interfacial bonding state, which is an important doping ratio for the optimisation of hot-melt processing performance, and provides structural guarantee for the subsequent moulding process and the enhancement of application performance.

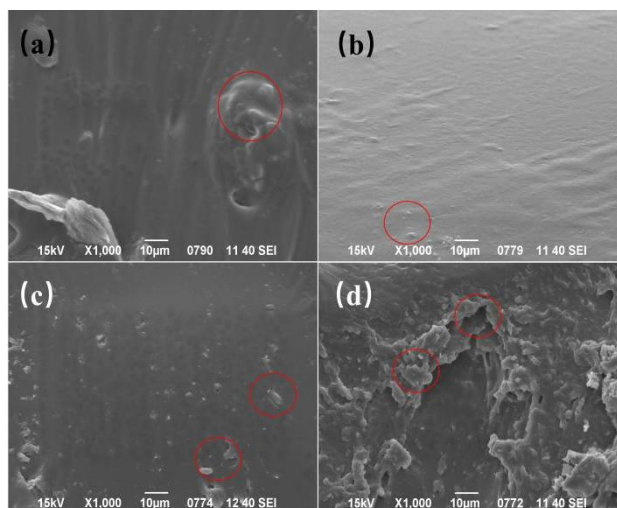


Figure 3 Microstructures of Different Samples by 1000x Electron Microscopy: (a) MMT-1, (b) MMT-2, (c) MMT-3, (d) MMT-4

3.2 FTIR

Figure 4 demonstrates the effect of different levels of montmorillonite (MMT) doping on the infrared spectra of enzymatically crosslinked starch (ECSS) materials, thus reflecting the changes in chemical structure during the hybridisation process. The comparison shows that the absorption peaks of the samples in specific wavelength bands changed significantly with the gradual increase of montmorillonite doping, indicating that the hybridisation process changed the interactions between the molecular chains of the starch molecules and the environment of the functional groups to a certain extent.

In the region of 3200-3600 cm^{-1} , all the samples showed strong broad peaks, which are the characteristic peaks of -OH stretching vibration, representing the presence of hydroxyl groups in starch. With the increase of MMT content, this absorption peak gradually showed a weak red shift and a slight decrease in peak intensity, indicating that some of the hydroxyl groups were involved in hydrogen bonding with the hydroxyl groups on the surface of the montmorillonite or the organic intercalating agent, which led to the reconfiguration of the original hydrogen bonding network between the molecules, thus enhancing the interfacial bonding between the substrate and the inorganic lamellae. In addition, multiple absorption peaks (e.g., C-O-C and Si-O correlation stretching vibrations) in the region of 1000-1200 cm^{-1} also undergo enhancement and splitting phenomena with the change of MMT doping amount, especially at 3.5g and 5g

MMT samples. This change may be related to the Si-O-Si structure of the MMT interlayers and the formation of novel interactions between them and the ether bonds in the starch, which further confirms that the introduction of the inorganic phase achieves effective hybridisation at the molecular level. The peaks around 900 cm^{-1} also show enhancement, suggesting that Si-O-Al or Si-O-Mg groups were introduced into the hybridised system, indirectly confirming that the montmorillonite structure was retained and successfully embedded in the starch matrix. The changes in IR spectra clearly reveal that the physical and chemical interactions between ECSS molecules and montmorillonite are gradually enhanced with the increase of the MMT doping ratio, and more complex and stable hydrogen bonding and chemical cross-linking structures are formed within the material. Among them, the samples with 1.5g and 3.5g MMT additions showed more coordinated changes in the characteristic peaks, which indicated that their structures were better hybridised and might have better performance in the subsequent performance tests.

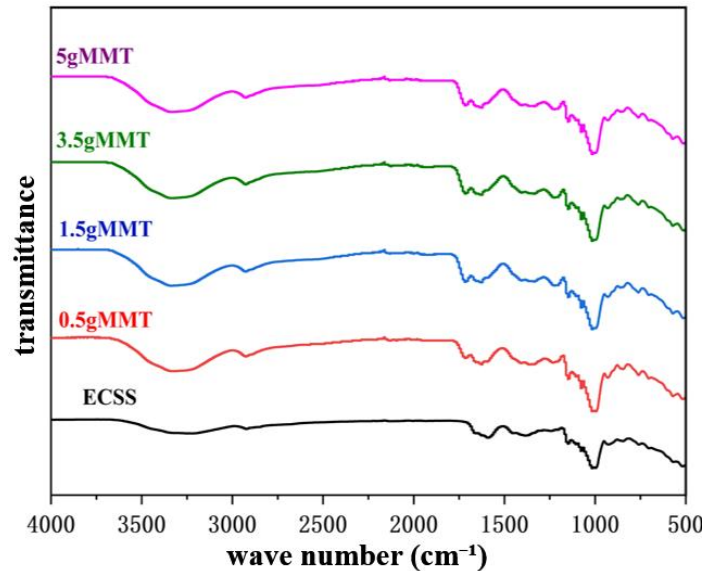


Figure 4 Infrared Spectra of Hybrid Samples of Starch Montmorillonite with Different Contents

3.3 TGA

According to the thermogravimetric analysis (TGA) data in Figure 5, the thermal stability of thermoplastic starch materials with different contents of montmorillonite (MMT) doping is shown. By comparing the original starch-based material (ECSS) with the composites with different amounts of MMT doping, it is evident that the thermal stability of the material is enhanced by the addition of MMT. The thermal degradation trend was approximately the same for all samples. Weight loss occurred in the range of $80\text{--}180^\circ\text{C}$, mainly due to evaporation of water from the composites. At further elevated temperatures, the maximum rate of weight loss for all samples occurred at approximately 300°C . Weight loss in this temperature range is usually associated with the removal of hydroxyl groups from the composites, dehydration reactions of oxygen-containing groups, and degradation of starch molecular chains.

The rate of thermal degradation of the samples changed as the MMT content increased. In particular, the thermal degradation curves of the composites became smoother at montmorillonite contents of 1.5 g and 3.5 g (MMT-2 and MMT-3), with lower rates of degradation processes compared to the pristine ECSS samples, which suggests that the addition of MMT improved the thermal stability of the materials.

In particular, the thermal degradation process of the material became slower with the addition of 5 g MMT (MMT-4), which showed better thermal stability. This suggests that higher content of montmorillonite can effectively improve the thermal degradation resistance of the composites, reduce the volatiles during thermal decomposition, and also enhance the high temperature resistance of the materials through the barrier effect of montmorillonite lamellar structure.

Overall, the addition of montmorillonite (especially in the range of 1.5 g to 5 g) significantly enhanced the thermal stability of starch-based composites and provided stronger support for the application of the material in high-temperature environments.

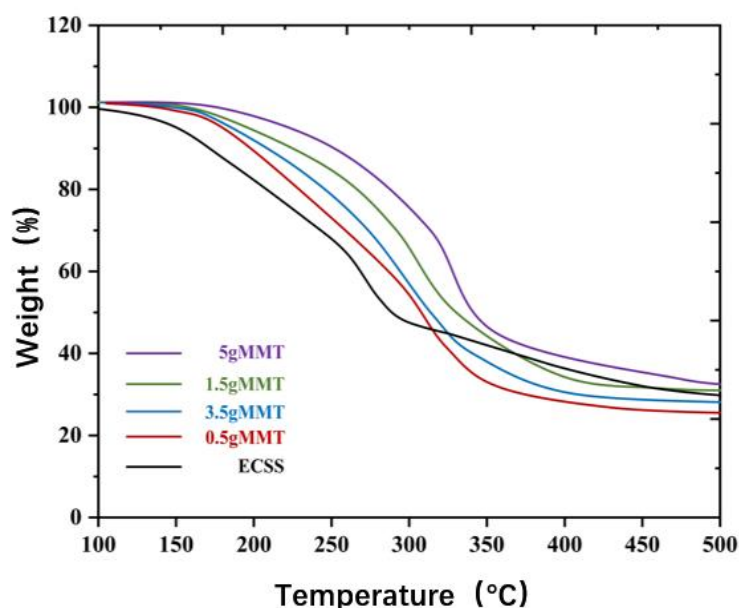


Figure 5 TGA Spectra of Different Samples

3.4 Mechanical Properties

From Figure 6, it can be seen that the tensile strength of the composites shows a trend of first increasing and then slightly decreasing with the increase of OMMT doping. The tensile strength of the matrix sample ECSS, which is not doped with OMMT, is only 1.12 MPa, which is a weak mechanical property. After the addition of 0.5 g OMMT (sample MMT-1), the tensile strength was elevated to 1.42 MPa, indicating that a small amount of OMMT has already been able to enhance the structural linkage between starch molecules and improve the overall strength. When the OMMT addition was further increased to 1.5 g (MMT-2), the material exhibited the highest tensile strength of 2.03 MPa, which is about 1.8 times that of ECSS. This indicates that at this ratio, the OMMT is more uniformly dispersed in the matrix, with obvious reinforcement, and a more desirable composite interfacial structure may have been formed. However, when the OMMT content continued to increase to 3.5 g (MMT-3) and 5 g (MMT-4), the tensile strength decreased to 1.84 MPa and 1.59 MPa, respectively, which is presumed to be due to the fact that high OMMT content tends to agglomerate in the starch matrix, resulting in the emergence of stress concentration points within the material, which weakened the reinforcing effect. This phenomenon indicates that the reinforcing effect of fillers is effective within a certain range, but excessive use will bring side effects instead. Therefore, the addition amount of OMMT needs to be reasonably controlled in the material design in order to exert the best reinforcing effect.

As far as elongation at break is concerned, the overall trend is similar to that of tensile strength, i.e., the performance is optimal when doped in the right amount and poor when doped too high or too low. The elongation at break of ECSS is 260.53%, which is at the basic level. The doping of 0.5 g of OMMT (MMT-1) resulted in a slight increase in elongation to 275.47%, indicating that the introduction of the filler resulted in an increase in the flexibility of the material. Continuing to increase the OMMT content to 1.5g (MMT-2), the elongation at break reached 310.39%, the highest value among all the samples. This indicates that at this ratio, there is good compatibility and better dispersion between OMMT and starch matrix, which helps in the slip of polymer chains and thus enhances the ductility properties of the material. When the OMMT incorporation was increased to 3.5 g (MMT-3) vs. 5 g (MMT-4), the elongation at break decreased to 296.26% vs. 280.36%, respectively, which is still significantly better than the unhybridised samples, but has decreased compared to the 1.5 g group. This decrease may be attributed to the uneven dispersion caused by the excessive fillers, which formed localised hard regions, limiting the ductile space of the molecular chains and thus affecting the tensile toughness of the materials.

Therefore, the introduction of OMMT effectively improved the mechanical properties of starch materials, and the enhancement was most significant when added in moderate amounts (e.g., MMT-2). However, when the addition amount exceeded a certain threshold, the material properties were inhibited instead.

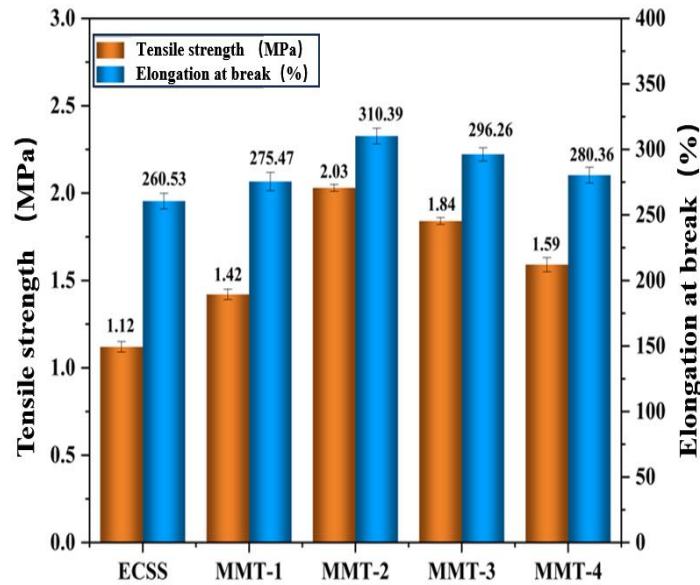


Figure 6 Mechanical Property Spectra of Different Samples: Tensile Strength, Elongation at Break

Figure 7 shows the Young's modulus of different samples, from which it can be seen that the Young's modulus of the thermoplastic starch composites shows a tendency to increase and then decrease with the addition of MMT. In the matrix sample ECSS without MMT addition, the Young's modulus was 77.3 MPa. After the addition of MMT, the Young's modulus increased significantly, especially at the addition of 1.5 g of MMT (MMT-2), the Young's modulus reached 135.23 MPa, which was about 75% higher than that of the matrix without MMT addition (ECSS). This change indicates that the addition of MMT effectively enhanced the rigidity of the composite and improved its mechanical properties. When the addition of MMT continued to increase to 3.5 g (MMT-3), the Young's modulus continued to increase to 129.75 MPa, indicating that MMT was well dispersed in the matrix and further enhanced the rigidity of the composite. However, when the addition of MMT was increased to 5 g (MMT-4), the Young's modulus instead decreased to 114.77 MPa. This trend suggests that too much MMT may lead to the aggregation of fillers, which affects the good bonding between the matrix and fillers, and thus reduces the rigidity of the composites. The dispersion of the filler and the interaction between the matrix have a great influence on the mechanical properties of the composites. The Young's modulus gradually increased with the increase of MMT addition, and the material rigidity was significantly enhanced especially at moderate additions (e.g., at 1.5 g). This suggests that the good combination and uniform dispersion of MMT with starch matrix promote the reinforcing effect of the composites. With the excessive addition of filler, the dispersion may deteriorate, leading to the problem of stress concentration within the material, which inhibits the improvement of Young's modulus.

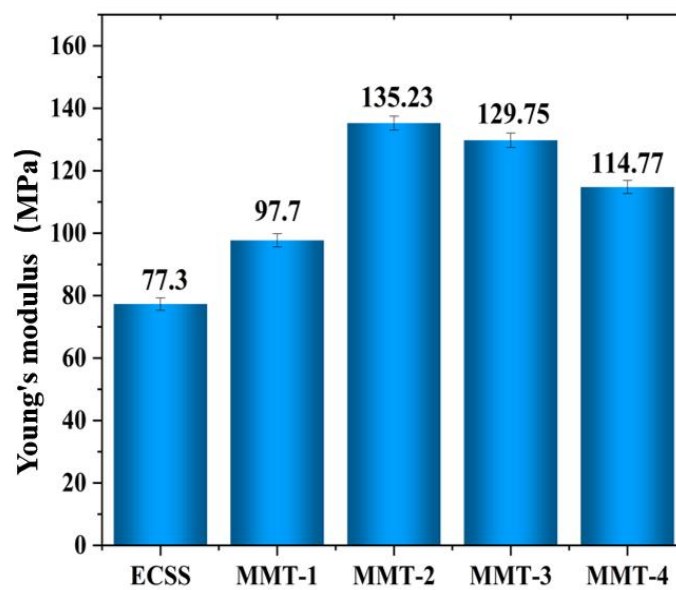


Figure 7 Young's Modulus of Different Samples

3.5 Water Vapour Transmission Rate

In order to assess the performance of the hybrid materials in terms of water repellency, the water vapour transmission rate (WVTR) of each group of samples was tested and the results are shown in Figure 8. The figure shows that the WVTR value of the original ECSS samples was $13.3 \times 100 \text{ g/m}^2\text{-24h}$, which is a high moisture permeability, indicating a weak barrier to water vapour. This may be related to the presence of a certain number of micropores and polar functional groups in the structure of the material itself, which makes it easy for water molecules to diffuse and migrate in the membrane layer.

The composites doped with different contents of OMMT showed some improvement in WVTR performance. The WVTR of the MMT-1 sample with 0.5 g of OMMT added decreased to $12.5 \times 100 \text{ g/m}^2\text{-24h}$, which preliminarily verified the effectiveness of montmorillonite in enhancing the barrier properties. With a further increase in OMMT addition, the MMT-2 sample corresponding to 1.5 g of OMMT showed optimal performance, with its WVTR value decreasing to $11.2 \times 100 \text{ g/m}^2\text{-24h}$, which was nearly 16% lower than that of the unhybridised sample. This significant improvement was attributed to the fact that the appropriate amount of OMMT formed a denser dispersion in the starch matrix, and the lamellar structure effectively elongated the water vapour penetration path and suppressed the formation of microporous structures to a certain extent, resulting in a tighter and more complete internal structure of the material. However, when the OMMT content continued to increase to 5 g (MMT-3) and 5 g (MMT-4), the WVTR values instead rebounded to 11.8×100 and $12.3 \times 100 \text{ g/m}^2\text{-24h}$, respectively. This trend suggests that excessive OMMT doping may trigger stacking and agglomeration between the lamellae, which generates structural defects within the hybridised system, such as microcracks or localised sparse regions, thus weakening the overall barrier performance.

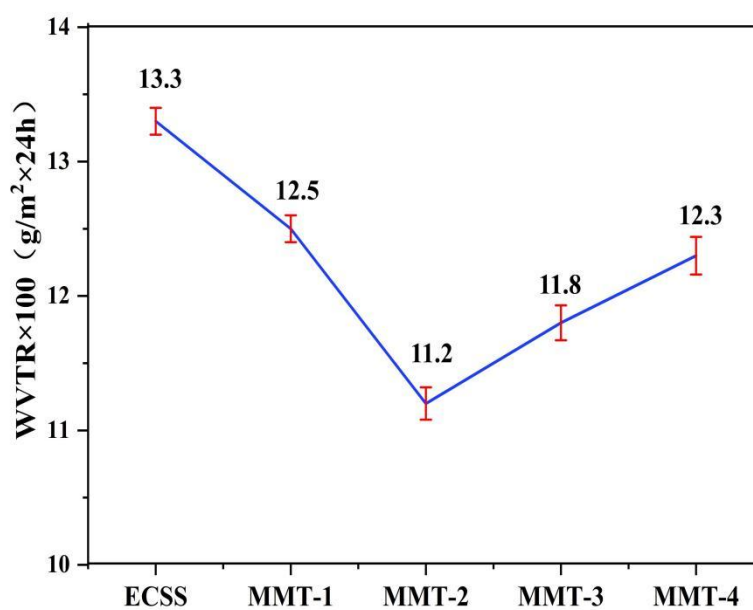


Figure 8 Water Vapor Permeability of Different Samples

3.6 Water Contact Angle Test

The water contact angle test is a common tool to evaluate the surface wettability and hydrophilicity of membrane materials. Figure 9 shows the water contact angle trends of ECSS and its hybridised samples with different additions of organo-montmorillonite (OMMT). The results show that the water contact angles of all the hybridised membranes were significantly higher than those of the original ECSS samples, indicating that the introduction of OMMT effectively improved the surface hydrophobicity of the membranes.

In the ECSS membrane without OMMT addition, the water contact angle was only 50.95° , showing typical hydrophilicity, which was closely related to the presence of a large number of free hydroxyl groups in the starch molecule. With the addition of OMMT, the water contact angle gradually increased and reached 58.63° for sample MMT-1 (addition amount of 0.5 g), indicating that even a small amount of filler doping could significantly inhibit the adsorption capacity of water on the membrane surface. Further increasing the addition amount to 1.5 g (MMT-2), the water contact angle reached the highest value of 68.47° , indicating that at this time the dispersion and binding between OMMT and the starch matrix were most ideal, and the lamellar structure of OMMT might form a dense barrier layer on the membrane surface, which partially obscured the exposure of the polar groups, weakened the affinity and adsorption of water molecules, and thus maximally enhanced the surface hydrophobicity. However, when the OMMT addition continued to increase to 3.5 g (MMT-3) vs. 5 g (MMT-4), the water contact angle slightly decreased to 63.79° vs. 59.52° , respectively, which might be related to the excess of filler leading to the stacking of the lamellae and the decrease of dispersion. After agglomeration of the lamellae in the membrane or on the surface, it is easy to produce structural defects such as microscopic depressions, holes, etc. These defects, on the contrary, provide a 'landing place' for the attachment and expansion of water droplets, which leads to the increase of the overall wettability of the surface of the membrane.

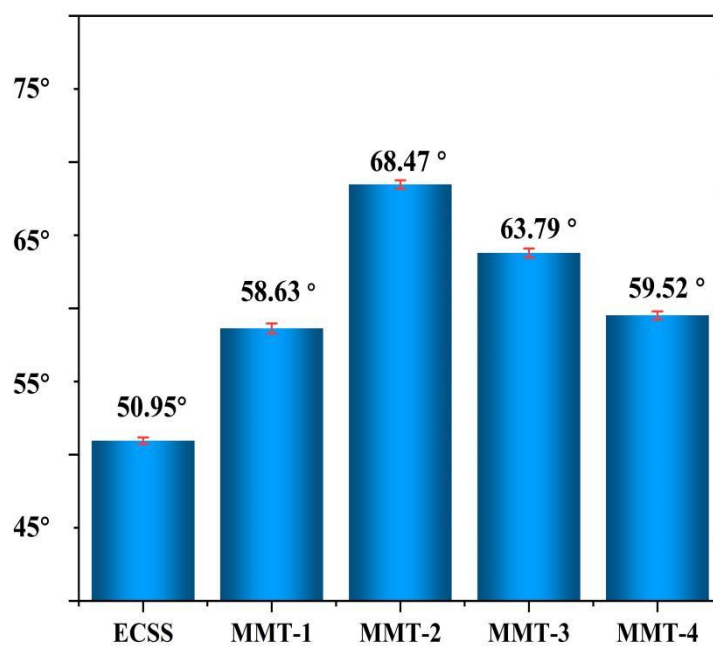


Figure 9 Water Contact Angle of Different Samples

4 CONCLUSIONS

In this study, the enhancement mechanism of organically modified montmorillonite (OMMT) in its heterogeneous modification process and its effect on the properties of composites were investigated using enzymatically cross-linked hot melt starch (ECSS). By controlling the addition amount of OMMT, a series of composites with uniform structure and stable properties were prepared, and the variation rules of mechanical properties, water contact angle, Young's modulus and thermal stability were systematically evaluated.

The experimental results show that the appropriate amount of OMMT (especially at 1.5 g addition) can significantly enhance the tensile strength and elongation at break of the composites, which are about 1.8 times and 19.1% higher than that of the matrix material ECSS, respectively. Meanwhile, the Young's modulus of the hybrid material is significantly increased and the onset temperature of thermal decomposition is delayed, indicating that the rigidity and thermal stability of the material are simultaneously enhanced. In addition, the increase of water contact angle reflects the enhancement of surface hydrophobicity, implying that the adaptability of the material in humid environment is improved.

However, when the filler addition exceeded a certain threshold (e.g., 3.5 g and above), the material properties showed a decreasing trend, which was presumed to be mainly caused by the aggregation of OMMT in the matrix leading to stress concentration and interfacial discontinuity. This phenomenon suggests that the reasonable control of filler ratio and dispersion state is the key to achieve the construction of high-performance starch matrix composites.

In conclusion, this study demonstrated the feasibility and effectiveness of the enzymatic cross-linking-OMMT hybrid system in enhancing the comprehensive performance of hot-melt starch, which provides a theoretical basis and experimental support for the application of starch-based biodegradable materials in the fields of green packaging, agricultural films and sustainable plastic substitutes. Future research can further focus on the structural regulation of the hybrid interface, the optimisation of the toughening mechanism and the stability evaluation of the composite system in complex environments, in order to promote its development towards engineering and industrialisation.

COMPETING INTERESTS

The authors have no relevant financial or non-financial interests to disclose.

REFERENCES

- [1] Wei Z, Wei Y, Liu Y, et al. Biochar-based materials as remediation strategy in petroleum hydrocarbon-contaminated soil and water: Performances, mechanisms, and environmental impact. *Journal of Environmental Sciences*, 2024, 138: 350-372.
- [2] Magaji S, Hussain I, Malaibari Z, et al. Catalytic Cracking of Liquefied Petroleum Gas (LPG) to Light Olefins Using Zeolite-Based Materials: Recent Advances, Trends, Challenges and Future Perspectives. *The Chemical Record*, 2024, 24(11): e202400110.
- [3] Guo C, Guo H J M. Progress in the degradability of biodegradable film materials for packaging. *Membranes*, 2022, 12(5): 500.

- [4] Li W, Liu Q, Zhang Y, et al. Biodegradable materials and green processing for green electronics. *Advanced Materials*, 2020, 32(33): 2001591.
- [5] Zhang X, Wang L, Xu J, et al. Effect of Starch Chain Structure and Non-Starch Components on the Hydrolysis of Starch by α -Amylase. *Starch - Starke*, 2022, 74(7-8): 2100107.
- [6] Kim R J, Kim H-S J F S, *Biotechnology*. Development and characterization of potato amylopectin-substituted starch materials. *Food Science and Biotechnology*, 2021, 30(6): 833-42.
- [7] Zhang C, Zhang P, Li Y, et al. Fully biodegradable, hydrophobic, enhanced barrier starch bio-composites with sandwich structure by simulating wood. *Industrial Crops and Products*, 2023, 197: 116603.
- [8] Massijaya S Y, Lubis M A R, Nissa R C, et al. Thermal Properties' Enhancement of PLA-Starch-Based Polymer Composite Using Sucrose. *Polymers*, 2024, 16(8): 1028.
- [9] Castillo L, López O, García M, et al. Crystalline morphology of thermoplastic starch/talc nanocomposites induced by thermal processing. *Heliyon*, 2019, 5: e01877.
- [10] Zain A H M, Wahab M K A, Ismail H J P B. Solid-state photo-cross-linking of cassava starch: Improvement properties of thermoplastic starch. *Polymer Bulletin*, 2018, 75(8): 3341-56.
- [11] Bergel B F, Osorio S D, da Luz L M, et al. Effects of hydrophobized starches on thermoplastic starch foams made from potato starch. *Carbohydrate Polymers*, 2018, 200: 106-14.
- [12] Jiun Y L, Tze C T, Moosa U, et al. Effects of recycling cycle on used thermoplastic polymer and thermoplastic elastomer polymer. *Polymers and Polymer Composites*, 2016, 24(9): 735-40.
- [13] Ouyang H, Jin D, He Y, et al. Effect of branched 1, 4-butanediol citrate oligomers with different molecular weights on toughness and aging resistance of glycerol plasticized starch. *International Journal of Biological Macromolecules*, 2024, 268: 131603.
- [14] Wang S, Zhang P, Li Y, et al. Recent advances and future challenges of the starch-based bio-composites for engineering applications. *Carbohydrate Polymers*, 2023, 307: 120627.
- [15] Paluch M, Ostrowska J, Tyński P, et al. Structural and thermal properties of starch plasticized with glycerol/urea mixture. *Journal of Polymers and the Environment*, 2022: 1-13.
- [16] Khan B, Niazi M B K, Hussain A, et al. Influence of carboxylic acids on mechanical properties of thermoplastic starch by spray drying. *Fibers and Polymers*, 2017, 18: 64-73.
- [17] Xiao H, Lin Q, Liu G Q J M. Effect of cross-linking and enzymatic hydrolysis composite modification on the properties of rice starches. *Molecules*, 2012, 17(7): 8136-46.
- [18] Xie J, Wei S, Xu X, et al. Preparation, Structure, and Properties of Enzymatically-Hydrolyzed Starch for Slowing Down the Retrogradation of High Starchy Foods. *Starch-Starke*, 2022, 74(3-4): 2100213.
- [19] Zhou G, Zhang X, Lei Z, et al. Dynamic imine crosslinking for waterproof starch plastic with tunable mechanical properties. *International Journal of Biological Macromolecules*, 2024, 282: 136872.
- [20] Yin P, Chen C, Ma H, et al. Surface cross-linked thermoplastic starch with different UV wavelengths: mechanical, wettability, hygroscopic and degradation properties. *RSC Advances*, 2020, 10(73): 44815-23.
- [21] Ning H, ZHANG Z-K, Yu-Hua L, et al. Spectroscopic Analysis of Chloride Ion-induced Structural Change of *Bacillus Amyloliquefaciens* α -Amylase. *Chinese Journal of Analytical Chemistry*, 2019, 47(10): e19130-e8.
- [22] Rajendran S, Radha C, Prakash V J I J o P, et al. Mechanism of solvent-induced thermal stabilization of α -amylase from *Bacillus amyloliquefaciens*. *International Journal of Peptide and Protein Research*, 1995, 45(2): 122-8.
- [23] Belsom A, Rappsilber J J C o i c b. Anatomy of a crosslinker. *Current Opinion in chemical Biology*, 2021, 60: 39-46.
- [24] Kapelko-Żeberska M, Zięba T, Pietrzak W, et al. Effect of citric acid esterification conditions on the properties of the obtained resistant starch. *Institute of Food Science and Technology*, 2016, 51(7): 1647-54.
- [25] Zhao Y, Zheng Z, Zhao Y, et al. Cross-linked modification of tapioca starch by sodium Trimetaphosphate: An influence on its structure. *Food Chemistry: X*, 2024, 23: 101670.
- [26] Noulis K, Frangopoulos T, Arampatzidou A, et al. Sodium Trimetaphosphate Crosslinked Starch Films Reinforced with Montmorillonite. *Polymers*, 2023, 15(17): 3540.
- [27] Compart J, Singh A, Fettke J, et al. Customizing starch properties: A review of starch modifications and their applications. *Polymers*, 2023, 15(16): 3491.
- [28] Ribeiro P L L, Figueiredo T V B, Moura L E, et al. Chemical modification of cellulose nanocrystals and their application in thermoplastic starch (TPS) and poly (3-hydroxybutyrate)(P3HB) nanocomposites. *Polymers for Advanced Technologies*, 2019, 30(3): 573-83.
- [29] Yang J, Li Y, Li X, et al. Starch-fiber foaming biodegradable composites with polylactic acid hydrophobic surface. *International journal of Biological Macromolecules*, 2024, 267: 131406.
- [30] Alves M J d S, Chacon W D C, Gagliardi T R, et al. Food applications of starch nanomaterials: a review. *Starch-Starke*, 2021, 73(11-12): 2100046.
- [31] Liao Y, Liu L, Wang M, et al. Preparation and properties of starch-based polyurethane/montmorillonite composite coatings for controlled-release fertilizer. *Polymer Composites*, 2021, 42(5): 2293-304.
- [32] Mardani T, Khiabani M S, Mokarram R R, et al. Immobilization of α -amylase on chitosan-montmorillonite nanocomposite beads. *International Journal of Biological Macromolecules*, 2018, 120: 354-60.
- [33] Qin Y, Wang W, Zhang H, et al. Effects of organic modification of montmorillonite on the properties of hydroxypropyl di-starch phosphate films prepared by extrusion blowing. *Materials*, 2018, 11(7): 1064.

- [34] Li J, Zhou M, Cheng G, et al. Fabrication and characterization of starch-based nanocomposites reinforced with montmorillonite and cellulose nanofibers. *Carbohydrate Polymers*, 2019, 210: 429-36.
- [35] de Freitas A d S M, da Silva A P B, Montagna L S, et al. Thermoplastic starch nanocomposites: sources, production and applications—a review. *Journal of Biomaterials Science, Polymer Edition*, 2022, 33(7): 900-45.